KERNFORSCHUNGSZENTRUM

KARLSRUHE

Juli 1976 KFK 2287

Institut für Neutronenphysik und Reaktortechnik
Projekt Schneller Brüter

Investigation of Heterogeneity Effects Arising in Fast-Thermal Test Loops

J. V. Lolich

GESELLSCHAFT
FÜR
KERNFORSCHUNG M.B.H.

KARLSRUHE

Als Manuskript vervielfältigt

Für diesen Bericht behalten wir uns alle Rechte vor

GESELLSCHAFT FÜR KERNFORSCHUNG M. B. H.

KARLSRUHE

KERNFORSCHUNGSZENTRUM KARLSRUHE

KFK 2287

Institut für Neutronenphysik und Reaktortechnik
Projekt Schneller Brüter

Investigation of Heterogeneity Effects Arising in Fast-Thermal Test Loops

José V. Lolich *

* Delegate from Comisión Nacional de Energia Atómica, Argentina

Gesellschaft für Kernforschung mbH., Karlsruhe

Investigation of Heterogeneity Effects Arising in Fast-Thermal Test Loops

ABSTRACT

The resonance self-shielding of different enriched uranium fuel element clusters in a 1/E spectrum has been studied experimentally and theoretically.

For the experiments metal uranium foils were used for direct measurement of the most important fission rate fine structures. An ARGONAUT reactor was used for the irradiation.

For the theoretical calculations the Monte Carlo code KAMCCO and the Multigroup Code WIMS were used. For all the studied geometries an excellent agreement exists between KAMCCO predictions and experiment. Application of the methods developed to the planned MOL-7C experiments has demonstrated the presence of considerable power gradients across the fuel pins if these high enriched test pins are irradiated in a thermal reactor despite the Cd shielding of the cluster.

Untersuchung von Heterogenitätseffekten in Brennstabbündeln

Zusammenfassung

Die heterogene Resonanz-Selbstabschirmung in Brennstabbündeln wurde für angereicherte Brennstäbe in unterschiedlichen geometrischen Anordnungen in einem 1/E-Spektrum experimentell und theoretisch untersucht.

Dazu wurden metallische Uranfolien in Brennstäbe zwischen die Tabletten eingelegt und in einem Argonaut-Reaktor bestrahlt. Aus der Aktivitätsverteilung auf den Folien wurde die Flußfeinstruktur bestimmt.

Für die Berechnung wurden der Monte Carlo Code KAMCCO und das Zell-Berechnungsprogramm WIMS verwendet. In allen Fällen ergab sich eine sehr gute Übereinstimmung zwischen KAMCCO Rechnung und Messung. Am Beispiel des Mol7C-Versuchseinsatzes wurde gezeigt, daß trotz eines Cadmium-Filters erhebliche Leistungsgradienten über einem Brennstab auftreten, wenn man Stabbündel mit hoch angereichertem Brennstoff in einem thermischen Reaktor einsetzt.

Acknowledgements

The present work was done during a one year fellowship granted by the International Atomic Energy Agency, under the auspice of the Comisión Nacional de Energia Atómica, Argentina.

This time was spent in the Kernforschungszentrum Karlsruhe at the Institut für Neutronenphysik und Reaktortechnik (INR) under the supervision of DP. M. Küchle, who suggested the subject of the present work and continuously provided guidance during its realization. I would also thank Dr. H. Würz for his invaluable and constant assistance. I am grateful to Dr. H. Borgwaldt for his valuable help.

Finally, the generous assistance from members of the staff of the SNEAK-Physik Department and INR during the performance of this work is acknowledged.

CONTENTS

List of Figures

1. Introduction

Because of the limited irradiation space available in fast reactors, the irradiation, of fast reactor fuel rods or rod bundles are often performed in thermal reactors, both for fuel performance and for safety tests. But when the relatively high enriched fuel rods of a fast reactor are placed into a thermal reactor environment a strong flux depression occurs which can lead to unacceptable power gradients. Therefore it is usual to separate the irradiation loop from the driver core by a cadmium filter, thereby suppressing the thermal neutron contribution. In the epithermal range the absorption cross sections are much smaller than in the thermal range and the flux depression in the loop can be substantially reduced by this technique. Unfortunately the fissile materials have large resonances in the epithermal domain for which the absorption rate shows a strong surface effect, leading to power gradients. This is not properly taken into account in standard multigroup calculations where group averaged cross sections are used. On the other hand the cell calculation codes which treat the resonance absorption properly do not give the azimuthal distribution of power in individual rods. But it is just the power gradient across the rod which causes additional stresses, bowing or eventually pin failure not protypic to fast reactor conditions.

Therefore the power distribution within rods of rod bundles irradiated by epithermal neutrons were investigated experimentally and theoretically for different bundle sizes and geometries. For the experiments an ARGONAUT reactor was available (STARK)/1/ and for the calculations the Monte Carlo code KAMCCO /2/ was used. Among the codes available in Karlsruhe KAMCCO has the unique capability to treat simultaneously complex geometries and detailed resonance cross section shapes.

Zum Druck eingereicht am 5.7.1976

It was the aim of the study to see whether a receipt can be found to determine approximately the power gradient across a rod also when such a tool is not available. Therefore the cell calculation code WIMS /3/ was used in parallel.

2. Experimental Techniques

Different enriched uranium fuel element clusters were irradiated and metal uranium foils were used for direct measurements of the most important fission rate fine structures.

By choosing lattices with simple geometry, errors of representation in the theoretical methods have been minimized. The desired distributions were experimentally obtained by irradiating the detector foils between the fuel pellets. The experimental techniques, results in standard errors of less than 1 %, for the relative fission rates.

2.1 Lattice arrangements

The main characteristics of the available fuel pellets were:

- composition: UO_2
- enrichment: U-235/U = 20 %
- diameter: 6.9 mm
- density (derived from weight and dimensions): 10.50 gr/cm^3

The fuel rods were clad with aluminium (0.5 mm thick) and its active length were aprox. 300 mm.

Fine structure measurements have been carried out in the following lattice arrangements:

Table 1: Parameters of the lattices

Lattice Number	Pitch (cm) T = triangular S = square	Number of fuel rods	Figure
1	1,64 *	13	2
2	0,9 T	7	3
3	0,9 S	9	6
4	0,9 S	16	7
5	1,0 T	30	8

* outer ring of 12 pins and one inner pin

For these lattice arrangements, pin to pin variations within each fuel cluster, ring to ring variations within each pin of the cluster and variations within the pins (including cross pin gradients), were experimentally obtained.

The first lattice arrangement, was built up in order to test the 1-D code RABBLE. For this lattice a simplified cylindrical configuration could approximately beusedin the calculation.

The lattices 2 to 4 were irradiated to test under clean conditions the ability of the WIMS and/or KAMCCO codes for computing the resonance self-absorption in square and triangular lattices. The lattice No. 5 was experimentally studied in order to test the Monte Carlo code KAMCCO for a lattice as complicated as the MOL-7C /5/.

The bundles covered with 0,5 mm cadmium were irradiated in the central channel (Fig. 1) of the thermal graphite zone, of the zero power Argonaut reactor ARK (ϕ_{ep} = $2x10^6$ n/cm^2sec). The detector foils placed between the fuel pellets, consisted of 93

weight percent U-235, their weight was in the range of 0,1 grams. They were irradiated between aluminium catcher foils (0,003 cm thick) to avoid parasitic activity contributions. The foils sets were placed in the designated rods through windows cut in the cladding, so that the rods and foils were aligned axially. The components of the foil pack were kept under slight compression by a spring located at the end of the pack.

After irradiation the foils were cut into concentric pieces with an extremely precise tool (a central disc, 4,2 mm diam. and one ring). - Finally it has to be mentioned that sometimes small pieces were cut out of the foils, in order to get detailed flux distributions in the fuel rods. The axial position of the foil in the cluster was determined with the aid of a fine red line painted over the foil.

2.2 Gamma counting of the fission product activity

The counting operation of the irradiated foils was done in the usual way by measuring the fission product gamma activity having energies greater than 660 keV. Counting was accomplished by an automatically operated sample changer and electronic apparatus. To exclude the complex decay law of the fission product activity, all foils of one irradiation were repeatively counted in forward and backward cycle. Normally the total counting period was 2 to 3 days.

Two counting channels were used, each comprising of:

I) a Na I (Tl) crystal in conjuction with a photo-multiplier and preamplifier

II) a linear amplifier

III) a discriminator

IV) two scalers in parallel

Detected numbers of events from the scalers were recorded by a typewriter and on paper tape for the two separate counting channels.

Each channel was set to accept gamma rays with energies greater than 660 keV, using a pulse height analyser, a Cs-137 gamma source ($E\gamma$ = 660 keV) and a pulse generator.

During the counting of each batch of irradiated foils an unirradiated foil and a foilholder without foil were included and the counts obtained were used for the total correction for natural activity and counter background. The additional counter background that can arise from the other foils which are present on the table of the automatic sample changer was found to be negligible.

After irradiation each foil was washed in acetone to remove possible radioactive contamination.

The output raw counting data on paper tape were fed to a computer and corrected for counter dead-time, background and foil sensitivity, than the mean counting rate for each sample and random counting error were obtained. The data from both counting channels were combined. Foils sensitivities were assumed to be proportional to their weights.

2.3 Sources of Experimental Error

2.3.1 Correction for U-238 fission contribution

In order to determine the U-238 fission contribution to the total activity of the irradiated foils one irradiation was carried out in which a depleted uranium foil (0.22 % enriched in U-235) and an enriched uranium foil (93 % enriched in U-235) were situated 5 cm from each other in the fuel pin. Both foils were sandwiched between 0,003 cm aluminium guard foils. The counting procedure was the same as that used for the main irradiations and similar corrections were applied. The correction factor /6/ to be applied to eliminate the U-238 fission contribution was found to be lower than 0,04 %.

2.3.2 Differential gamma ray absorption in the foils

A correction was applied to allow for the differential gamma ray absorption by the foils due to their different thicknesses. It was determined experimentally by irradiating a foil (93 % enriched) and counting its gamma activity above the 660 keV bias level with various thicknesses of unirradiated foils between the irradiated foil and the detector. From this measurements a gamma-attenuation coefficient was determined which was then applied for the gamma-self attenuation correction in the foils.

The measured variation of count rate with absorber-thickness was found to be (o.60 ± 0.02) % for 0.01 mm.

2.3.3 Variations of the detector efficiency with the foil geometry

To study the variations in the efficiency of the Na I (Tl) detectors due to the different sizes of the foils (outer ring and inner disc or 1/4 of the outer ring and 1/4 of the inner disc) a foil covered with 1 mm cadmium was irradiated in a flat flux. After irradiation the foil was cut and the gamma-ray activitiesof each piece were determined in the usual way. The differences for the counting rates were in all the cases lower than the statistical error (0.3 %).

2.3.4 Variations in the sensitivity and discrimination level of the counting apparatus

To study these variations a Cs-137 gamma source of low activity was placed in the counting apparatus, as the gamma peak of this source is 660 keV, lower variations in the sensitivity and/or discrimination level will give higher variations in the counting rate. For one day of measurement in period as short as the one used in the main measurement no differences were observed in the counting rates.

In view of the lower count rates of the irradiated foils it was not expected to get gain shift with the count rate of the different foils.

2.3.5 Error in the fission rate measurements

I)	random errors in counting	0,5 % *
II)	errors in the foil weights	5×10^{-3} %
III)	different gamma ray absorber in the foils	1×10^{-2} %
IV)	variations in the efficiency of the detectors with the foil shape	0,3 %
V)	correction for U-238 fission contributions	4×10^{-2} %
Total error less than		1 %

* function of the measured foil activity

3. Lattice calculations

The calculations for the experimental set-ups were performed with the codes RABBLE /4/, WIMS /3/ and KAMCCO /2/.

3.1 Code RABBLE

In the RABBLE calculations the reactor cell (slab or cylindrical) is divided into regions and the energy range of interest is divided into many narrow groups. The neutron has then only one collision within a fine group and an integral transport theory formulation based on first flight escape and transmission probabilities is used. The integral equations are solved numerically using the escape probabilities from one region to another in the reactor lattice.

The lattice is treated with cosine currents impinging on the boundary.

The energy range covered in the RABBLE calculations was from 0,5 eV to 1000 eV. The KEDAK /7/ data set was used with 41 s-wave resonances and 14 p-wave resonances for U-238 and 204 s-wave resonances for U-235. Calculations were made with and without multilevel parameter treatment of resonances and with different lower cut-off energies. These variations gave effects smaller than 1 % in the computed ratios.

In view of the fact that RABBLE is a 1-D program, it was used only for the lattice No.1, for which the homogenization of the outer ring of 12 pins was possible.

In order to test the cross sections used in RABBLE, a comparison was made with the BNL-325 data for U-235 and U-238 in the energy range between 0,1 eV to 150 eV. In addition the infinite dilute resonance integrals were checked against the results obtained by Klunker /8/. In all the cases an excellent agreement was achieved.

3.2 The WIMS code

The multigroup code WIMS has been developed at Winfrith, to compute reactor lattice parameters. Its performance has been tested by many authors essentially in the thermal energy range /9/.

The principal geometric options deal with regular arrays of rods or clusters of rods. The resonance energy range is covered by 13 groups between 4 eV and 9118 keV, and its treatment is based on equivalence theorems /3/. First, a spectrum calculation is carried out, using all groups but only a few regions. The main transport calculation follows, which normally is done with less than the full number of groups, therefore spectra calculated for the different regions of the cell, are used to condense the cross sections to the few group structure. The main approximation introduced in WIMS in the resonance region above 4 eV, is the use of the "f-factor" corrected multigroup data /10/.

WIMS was run with the CLUSTER geometrical option and the PIJ-PERSEUS routine for the main transport calculations. The experimentals set-up were modeled without approximations in an airchannel of a graphite cell of 40 cm diameter.

3.3 Code KAMCCO

The Karlsruhe Monte Carlo code KAMCCO has been recently developed essentially as an instrument for analyzing fast neutron experiments. The natural approach choosen was to use a good model of the neutron physics involved, even at the cost of some increase in computation time and to avoid many of the approximations usually accepted in reactor computation.

Three dimensional systems with divisions into regions can be calculated describing exactly the experimental assembly studied. Nuclear data sets were prepared from the KEDAK data file /7/. During the random walk cross sections are computed on per isotope basis from data in core storage. For each isotope and cross section type a specific energy grid is used to perform a linear interpolation in the non-resonance regions. Inelastic scattering is described at discrete levels or at high energy through the evaporation model. Elastic scattering retains first order anisotropy in the center of mass system and involves transformation to the laboratory system. For low energies the cross sections for the two uranium isotopes are computed from a limited number of single level Doppler-broadened Breit-Wigner resonances. For U-235 this model is used below 46,5 eV, for U-238 below 1000 eV.

For the calculations performed with KAMCCO the experimental set-up was modeled as an air-fuel channel in a square graphite cell of width 40 cm with reflective outer boundaries. In general neutrons were injected isotropically with energies between 900 and 2000 eV at a central point of the graphite zone. The assumed lattice width and the source parameters guaranteed a satisfactory 1/E spectrum at the cell boundary. KAMCCO was run with the censustime option and an adapted collision routine, that treats fission as a pure removal reaction. Neutrons below 0,5 eV were removed by an absorbing pseudomaterial.

To decrease the computing time the calculations with KAMCCO were performed without the aluminium cans. WIMS calculations performed with and without the cans, gave effects in the computed fission rate less than 0,5 %.

4. Results

4.1 Lattice No. 1 (Fig. 2)

As a first approach a bundle with an outer ring of 12 pins and one inner pin was used.

The quantities measured and calculated were:

R_1 = ratio of the U-235 fission rate densities of the central pin and an outer pin,

R_2 = the same ratio for an inner disc and an outer ring of the central pin,

R_3 = the same ratio for an inner disc and an outer ring of an outer pin.

The results are summarized in the table of Fig. 2.

A simplified approximation (configuration B) was needed for calculations with the RABBLE code; this treats the outer ring of fuel pins as a homogenized ring zone with a suitable reduced smear density. The simplified cylindrical configuration was as follow:

$0 \leqslant r \leqslant r_1 = 0{,}345$ cm, material 1 (UO_2, 20 % enriched), $\rho_1 = 10{,}50$ gr/cm^3

$r_1 \leqslant r \leqslant r_2 = 1{,}297$ cm, air,

$r_2 \leqslant r \leqslant r_3 = 1{,}987$ cm, material 1, but with an equivalent reduced smear density, $\rho = \rho_1 \times 0{,}63$,

$r_3 \leqslant r \leqslant r_4$ = 5 cm, air

$r_4 \leqslant r \leqslant r_5$ = 50 cm, graphite.

With WIMS and KAMCCO two configurations have been investigated. The first one is equivalent to the RABBLE configuration. The second configuration (configuration A) treated the outer ring of fuel pins correctly, without homogenization.

One should note the difference between the true configuration A and the simplified B and the large deviation of the RABBLE R_1 value from experimental and WIMS-KAMCCO results. This large deviation led to make additional calculations to check the reliability of the methods used in the RABBLE code.

Firstly, free parameters in the RABBLE code, which determine, e.g. the spatial and energy grids were changed on a wide scale but without any significant influence.

Secondly, the influence of an assumption made in the RABBLE code was tested /11/. Namely that all partial currents J^+, J^- across a region boundaries have a cosine angular distribution. For this purpose a test modification was introduced into the Monte Carlo code KAMCCO, enforcing the same cosine distribution on all neutrons crossing region boundaries (modified KAMCCO in table of Fig. 2), but it shows an effect, which is far too small to explain the deviation of RABBLE by this assumed angular distribution.

Thirdly, the results obtained from KAMCCO and WIMS agree rather well with the experiment. The conclusion at this stage is that the available version of the RABBLE code and/or data can, for unexplained reasons, not be realiably applied.

The difference between the homogenized and the correct geometrical model seems acceptable, the gaps between the outer pins constitute about 18 % of the circumference. Independent runs, for the other geometries studied, confirmed that the homogenization trends to accentuate the fission rate depression in the central rings.

4.2 Lattice No. 2 (Fig. 3, 4 and 5)

This was the lattice for which more detailed experimental fission rates were obtained. It enabled a check of the experimental procedure by comparison of the results obtained for symmetrical positions in the fuel pins (Fig. 3), the agreement between such positions was excellent.

The experimental results for the fine detail fission rate could only be compared with the results obtained with the Monte Carlo code KAMCCO, which is able to accept a geometry as complicated as one might wish. In order to check that the disagreement between the experimental results and the KAMCCO results does not show a systematic deviation a second calculation was made (with KAMCCO), maintaining the same input data but changing the source position, so that both runs were independent. The resulting agreement between KAMCCO and experiment is excellent (Fig. 4).

The agreement between KAMCCO and/or WIMS and the experiment for the ratios that are possible to compute with WIMS also is good (Fig. 5).

4.3 Lattices No. 3 and No. 4 (Figs. 6 and 7)

In order to check the accuracy of the codes for other geometrical configuration two lattices with square array were measured.

In general the agreement between theory and experiment is acceptable.

It seems that the fission rate depression in the fuel pins computed by WIMS trends to be insensitive to the pin position in the cluster but in relation to the quoted errors the difference between WIMS results and experiment is not high enough to use the numerical value of the difference.

4.4 Lattice No. 5 (Fig. 8)

In order to test the Monte Carlo code KAMCCO for lattices as complicated as the MOL-7C /5/, an irradiation was made for a lattice of 30 pins with the same geometrical configuration of the MOL-7C, but with the available fuel pellets (UO_2, 20 % enriched). First calculations were made with the multigroup code WIMS which showed that the influence of the sodium moderater in the lattice gives no differences in the computed fission rate (table 2). Thus the simplest one, namely air, was used in the experimental arrangement.

Table 2 Lattice No. 5 - WIMS-calculations (Fig. 8)

Moderator	FR_1	FR_2	FR_3	FR_4
air	0,8921	0,9527	0,9860	1,0850
Al	0,8958	0,9523	0,9848	1,0841
Na	0,8961	0,9526	0,9850	1,0835

Note: The fission rates per pin were normalized to an average value of 1.0000 for the 30 pins arrangement.

The lattice irradiation and foils activities determination were done in the usual way. The results are given in the table of Fig. 9.

An excellent agreement exists between KAMCCO predictions and experiment for all the computed fission rates so that this code predicts events in the epithermal energy range in an excellent manner.

With WIMS a good agreement is obtained for the pin-pin variations across the lattice, though not so good agreement occurs for the flux depression across a pin, which seems to be calculated independent to the pin position in the lattice. For the outer pin WIMS underestimates the fission ratio depression between the inner disc and the outer ring by up to 4 %.

4.5 Lattice MOL-7B

The agreement between KAMCCO predictions and the experimental results for the lattice No. 5 shows that KAMCCO computes the flux depression for a lattice (20 % enriched) as complicated as the MOL-7C in an excellent manner, but in view of the high enrichment of the MOL-7C lattice (90 % for the inner pins), it was desirable to compare in addition, KAMCCO results with experiments for a relatively high enriched lattice, therefore calculations were carried out for the MOL-7B /12/ lattice (Fig. 10), for which power density distributions with the track recorders technique have been obtained at Mol. The main characteristics of the MOL-7B fuel pins are:

- outer diameter of the clad fuel pins: 6,0 mm
- cladding: stainless steel, 0,38 mm thick
- number of pins: 18
- PuO_2 content: 30 %
- U-235 enrichment: 70 %

- linear density of the fuel: 1,92 g oxide per cm
- pitch: 8,0 mm
- moderator: Na

The cadmium screen surrounding the loop has an outer diameter of 76 mm.

The experimental results /12/ and the results computed with KAMCCO are given in the table of Fig. 10 and in Fig. 11. With KAMCCO the fission ratio between the surfaces "a" and "i" also was obtained (Fig. 10). The result obtained was R = 0,74±0,03, which is in good agreement with the experimental fission ratio /12/: R = 0,70±0,02. The conclusion is that there is an excellent agreement between KAMCCO and experimental results for lattices as complicated as the MOL-7B and/or MOL-7C.

4.6 Lattice MOL-7C (Fig. 12)

Heterogeneity effects may play an important role in experimental set-ups consisting of a fast test loop inserted into a thermal driver zone. One example is the planned MOL-7C /5/ experiment in which a test cluster of enriched uranium fuel elements is going to be irradiated in the BR-2 reactor. The driver zone acts essentially as a neutron source, which shows a 1/E spectrum down to the cadmium cut-off energy of 0,5 eV. This fact gives, compared to fast reactors, an abnormally large weight to low energy neutrons, which may show heterogeneous resonance self-shielding.

Calculations for slightly larger pin diameters showed that due to azimuthal stresses the maximum permissible power gradient is 20 % across a pin diameter /13/.

The fuel pin bundle of the MOL-7C experiment consists of thirty stainless steel clad UO_2 pins without burn-up (Fig. 12). The main characteristics of the fuel pins are:

- outer diameter of the clad fuel pins: 6,0 mm
- cladding: stainless steel 4970, 0,38 mm thick
- fuel composition: UO_2
  U-235/U: 90, 80, 65 atom %
- linear density of the fuel: 1,929 g oxide per cm
- pitch: 7,9 mm.

It was not possible to compute the MOL-7C pin bundle with the code WIMS since this program gives errors in the resonance cross section calculations for fuel enrichments greater than 20 % (with the CLUSTER option).

For the KAMCCO calculations the MOL-7C pin bundle was modeled without the stainless steel cans and without the different materials surrounding the bundle; due to the following reason:

I) Each material present in the geometry defines at least two new surfaces. This increases the large computing time of the Monte Carlo calculation, thus one should try to define a geometry as simple as possible.

   In view of the cans small volume in the lattice their contribution to error is assumed to be small and with exception of a tungsten plug insulation of 1 mm, the surrounding materials have no-resonance cross sections (Al, Nb, He, H_2O, Na and stainless steel) in the energy range of interest.

II) Some of the surrounding materials (W, Nb, He) are not available in the program data set.

In order to check the influence in the computed fission ratio of a resonance material, an additional calculation was made with an U-238 plug (with an equivalent thickness to the tungsten one). The results show small effects in the computed fission ratios (table 4).

Previous calculations /5/ for the MOL-7C bundle have been carried out in order to obtain the U-235 enrichments needed to have a flattest radial fission density. The calculations were made for the real geometry with the aid of the two-dimensional four-groups transport code DIAMANT.

From the good agreement achieved between the results reported in /5/ and KAMCCO calculations (table 3) for the total fission rate per pin ; the conclusion is that the approximation introduced in KAMCCO calculations are justified.

Table 3 MOL-7C fission rates (Fig. 12)

Method	FR_1	FR_2	FR_3	FR_4
Report MOL-7C/2/	1.001	0.967	1.024	1.004
KAMCCO without U-238 plug	0.963 ±0.016	0.972 ±0.015	1.037 ±0.016	1.014 ±0.013
KAMCCO with U-238 plug	0.986 ±0.016	0.985 ±0.015	1.027 ±0.014	1.001 ±0.011

Note: The fission rates per pin were normalized to an average value of 1.000 for the 30 pins.

As can be seen the deviation from the average value of 1.000 is very small and does not exceed 4 %.

From the results obtained with KAMCCO it was also possible to compute the fission ratios for each pin (R = fission rate A/ fission rate B; Fig. 12) which show heterogeneity effects greater than 14 %.

Table 4 MOL-7C fission ratios (Fig. 12)

KAMCCO	R_1	R_2	R_3	R_4
with U-238 plug	0.945 ±0.024	0.919 ±0.022	0.868 ±0.020	0.871 ±0.016
without U-238 plug	0.947 ±0.025	0.922 ±0.024	0.872 ±0.023	0.876 ±0.017

Rj = (fission rate A)/(fission rate B); j = 1,2,3,4 (Fig. 13)

A new calculation was made with KAMCCO in order to obtain the fission ratio between the surfaces "a" and "i" (Fig. 12). The result obtained was R = 0.77±0.03 which gives a heterogeneity of 26 %.

From these results and from the relation:

$$FR \sim \Sigma_f \phi \sim \sigma_f e\phi \qquad \text{(e = enrichment of the fuel pin)}$$

it is possible to obtain approximately the flux distribution across the pins (Fig. 13) which shows a heterogeneity effect of higher than 25 % for the outer pins, a value higher than the maximum permissible /13/. The obtained results show the importance of taking into account the detailed fission rate distribution across the pins of a bundle to be irradiated in a 1/E neutron spectrum down to the cadmium cut-off energy.

5. Approximate method for computing fission ratios

From the experimental results obtained for the fission ratio between the inner disc and the outer ring of the lattices with square array (lattices No. 3 and No. 4) it seems that the flux depression across the fuel pins is independent of the number of pins in the lattice.

Table 5 Fission ratio for the lattices No. 3 and No. 4 (Figs. 6 and 7) (CPU time = 60 minutes for each lattice)

	$R_A=FR_1/FR_2$	$R_B=FR_3/FR_4$	$R_C=FR_5/FR_6$
Lattice No. 3	0,973±0,005	0,963±0,005	0,953±0,005
Lattice No. 4	0,974±0,006	0,963±0,008	0,954±0,008

Due, that the "unit cell" is in this case a square one, it seems possible to consider the cell, formed by two types of surfaces: "a" and "b".

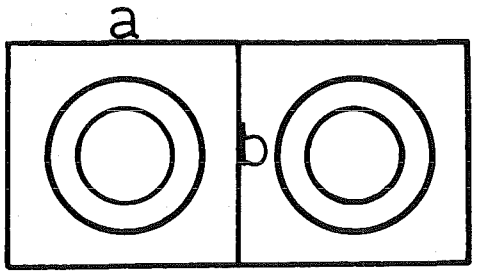

"a" free surface

"b" boundary surface

From the fission ratios R_A and R_B it is possible to obtain the value of the contribution of the surfaces "a" and "b":

$R_A = 4 \times b$; $b = 0,2433$

$R_C = 2 \times b + 2 \times a$; $a = 0,2333$

using these values for compute R_B:

$R_B = 3\ b + a = 0,963$

which is in excellent agreement with the real one ($R_B = 0,963 \pm 0,005$).

The same fission ratio was computed with KAMCCO for the simplest geometrical configuration; a lattice of four pins with the same enrichment, pin diameter and pitch. This geometry is a simple one, so the results obtained in less computing time are more precise. The fission ratio obtained between the inner disc and the outer ring of a pin was: (CPU time = 30 minutes)

$$R = 0{,}951 \pm 0{,}006$$

which is in excellent agreement with the respective fission ratio of the lattices No. 4 and No. 5 ($R_C = 0{,}953 \pm 0{,}005$). The conclusion at this stage is that for computing the fission ratio of a geometrical configuration in a 1/E spectrum it is enough to compute the value of the contribution due to the different types of surfaces of the unit cell, for the simplest geometrycal configuration, with the same enrichment, pitch and pin diameter.

To verify this assumption the different "unit cell surface contributions"for the lattice No. 5 were computed. To obtain these values the calculation of two simple geometries was necessary (Fig. 14). From these,it is possible to obtain the value of "a", "b" and "c":

$R_A = 6 \times a$; $a = 0{,}1624 \pm 0{,}0012$

$R_B = 3 \times a + 3 \times b$; $b = 0{,}1520 \pm 0{,}0011$

$R_C = 3 \times b + 2 \times a + 1 \times c$; $c = 0{,}1670 \pm 0{,}0050$

Applying the values of "a", "b" and "c" to the reallattice (Fig. 8)

$R_1 = (FR^C/FR^D)_1 = 1 \times c + 5 \times a$

$R_2 = (FR^C/FR^D)_2 = 6 \times a$

$R_3 = (FR^C/FR^D)_3 = 5 \times a + 1 \times b$

$R_4 = (FR^C/FR^D)_4 = 3 \times a + 3 \times b$

one obtains the results of table 6.

Table 6 Fission ratio for the lattice No. 5 (Fig. 8)

	$R_1=FR_1^C/FR_1^D$	$R_2=FR_2^C/FR_2^D$	$R_3=FR_3^C/FR_3^D$	$R_4=FR_4^C/FR_4^D$
This approximation (1) (KAMCCO)	0,979±0,008	0,974±0,007	0,964±0,006	0,943±0,005
Real geometry (2) (KAMCCO)	0,982±0,014	0,972±0,012	0,970±0,012	0,940±0,009
Experiment	0,972±0,009	0,967±0,008	0,963±0,007	0,944±0,007

(1) (CPU) time = 2 x 20 minutes (2) (CPU) time = 60 minutes

The results obtained by the use of this approximate method are in excellent agreement with KAMCCO and/or experiment results for the real geometry, so that this approximation is for the studied cases reliably applied.

From the obtained results it is possible without a new calculation to compute the fission ratio for the same lattice (lattice No. 5), but with 18 pins in the outer ring:

$R = 4 \times a + 2 \times b = 0,954 \pm 0,005$

or for the same lattice with a pin in the center:

$R = 6 \times a = 0,974 \pm 0,007.$

6. Conclusions

Measurements and calculations have been performed in order to test the available computational methods for computing detailed fission rates of uranium fuel element clusters in a 1/E spectrum down to the cadmium cut-off energy.

The conclusions obtained are:

I) The available version of the RABBLE code and/or data does for unexplained reasons not give good results.

II) The ring to ring fission ratio densities within a pin computed with WIMS trend to be insensitive to the pin position in the cluster.

III) There is an excellent agreement between the Monte Carlo code KAMCCO and the experimental results, so that this code predicts events in the epithermal energy range in a satisfactory manner.

IV) It was confirmed that the homogenization trends to accentuate the fission rate depression in the central pins. When homogenization was done an axcellent agreement between WIMS and KAMCCO was achieved.

V) Applications of the methods developed to the planned MOL-7C experiment have demonstrated the importance to take into account hetereogenity effects in experimental set-ups consisting of a fast test loop inserted into a thermal driver zone.

7. References

/1/ Meister H., et.al.
KFK 217 (1964)

/2/ Arnecke G., et.al.
KFK 2190 (1976)

/3/ Askew J., et.al.
J. Brit. Nucl. Energy Soc. 5, 564 (1966)

/4/ Kier P., Robba A.
ANL 7326 (1967)

/5/ MOL-7C experiment: unpublished (1975)

/6/ Bigham C., et.al.
AECL 1186 (1961)

/7/ Hinkelmann B., et.al.
KFK 1340 (1970)

/8/ Klunker J.
KFK 1879 (1973)

/9/ Chawla R.
J. Nucl. Energy, Vol. 27, pp. 797 (1973)

/10/ Kidman R., et.al.
Nucl. Sci. Engng., 48, 189 (1972)

/11/ Borgwaldt H. and Lolich J.
KFK 1275/4 (1976)

/12/ Debrue J., et.al.
BGL 488 (1974)

/13/ Küchle M.: Private Comunication

METHOD OF MOUNTING FOILS IN THE TEST CELL

Fig: 1

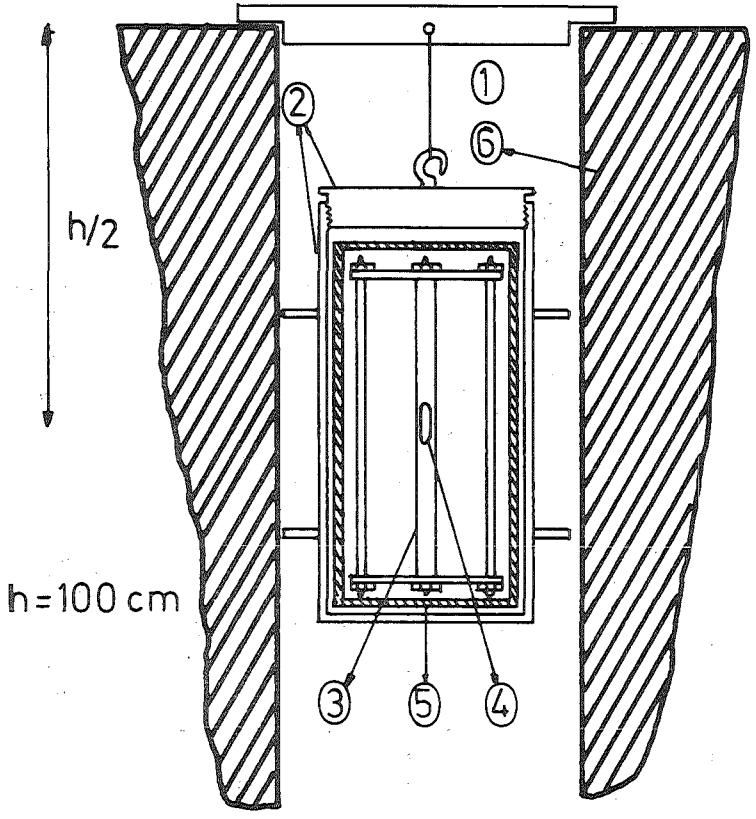

1 - center channel ARGONAUT reactor

2 - aluminium support

3 - fuel rod

4 - foil window

5 - cadmium shielding

6 - graphite

SECTION OF THE TEST CLUSTER

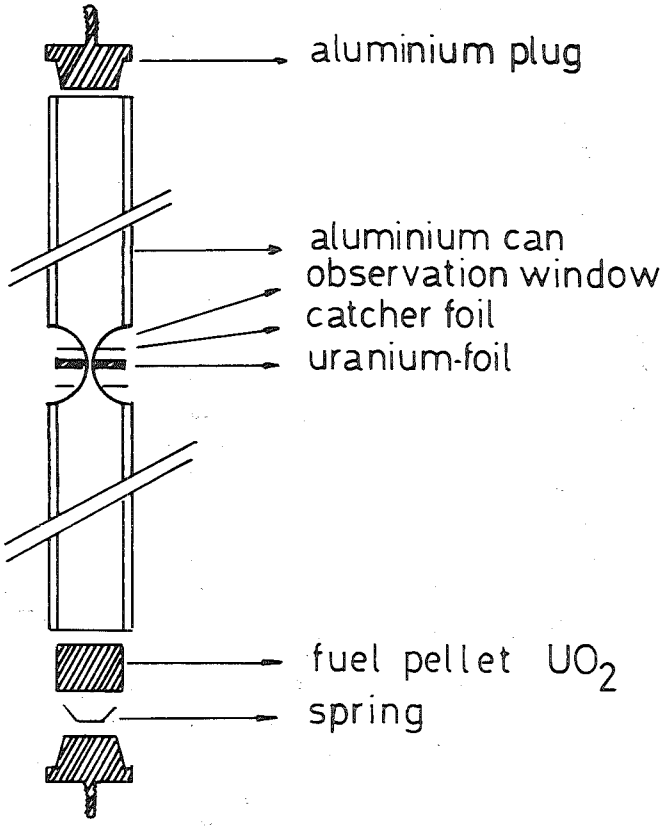

SECTION OF THE TEST ROD

LATTICE Nº1

FIG: 2

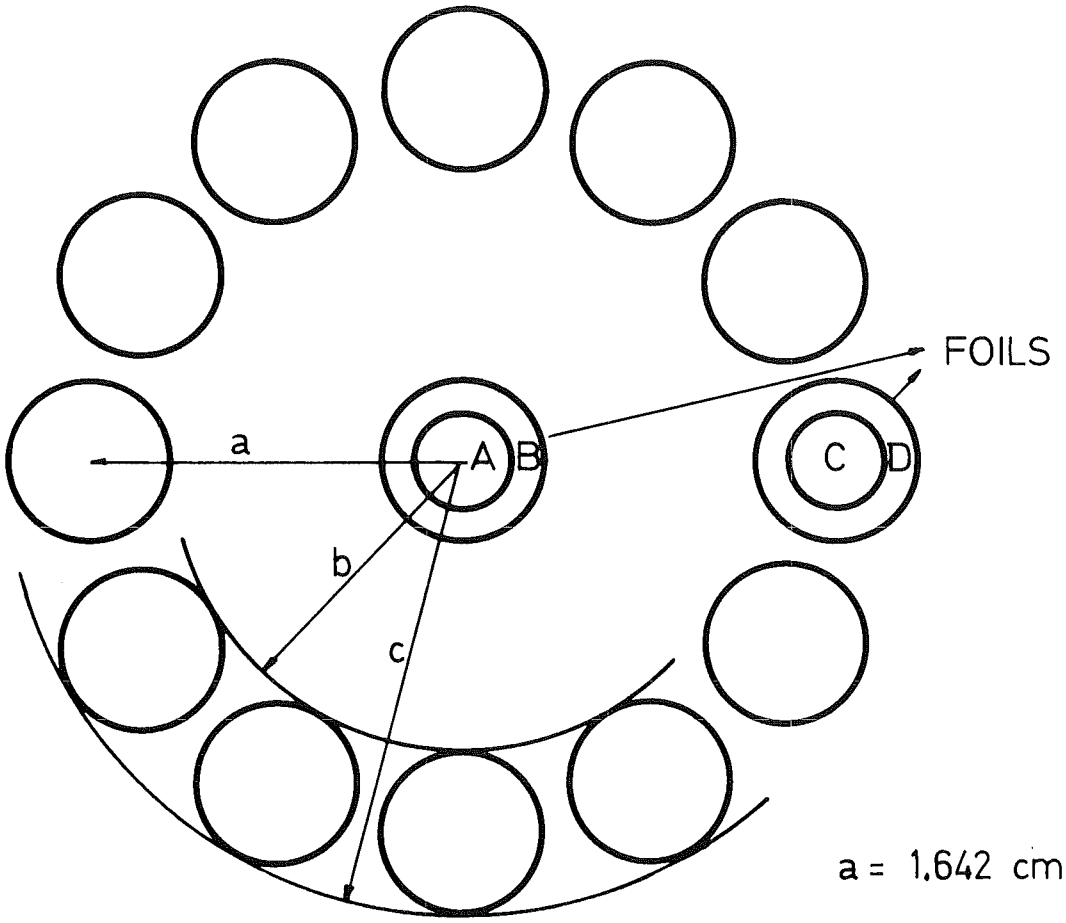

a = 1.642 cm

b = 1.297 cm

c = 1.987 cm

Method	Configurac.	R_1	R_2	R_3
Experiment	A	.95±3%	.95±2%	.94±2%
WIMS	A	.96	.95	.97
KAMCCO	A	.94±2.0%	.93±2.0%	.95±.6%
WIMS	B	.93	.95	
KAMCCO	B	.90±2.0%	.93±2.0%	
KAMCCO modif.	B	.88±1.8%	-	
RABBLE	B	.81	.95	

$$R_1 = \frac{FR_{A,B}}{FR_{C,D}} \qquad R_2 = \frac{FR_A}{FR_B} \qquad R_3 = \frac{FR_C}{FR_D}$$

LATTICE Nº2

FIG: 3

Experimental verification

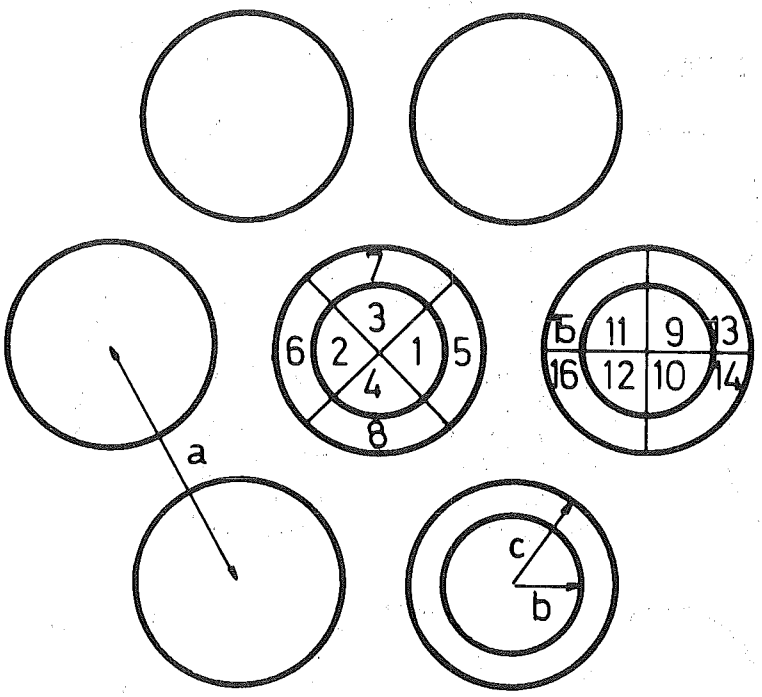

UO_2 (20%)

a = 0.9 cm

b = 0.211 cm

c = 0.345 cm

Position	Fission Rate °	Error
1	0.862±0.009	
2	0.868±0.008	0.7 %
3	0.855±0.012	
4	0.855±0.010	-
5	0.887±0.007	
6	0.893±0.008	0.7 %
7	0.895±0.004	
8	0.895±0.005	-
9	0.931±0.005	
10	0.939±0.005	0.9 %
11	0.898±0.005	
12	0.891±0.005	0.8 %
13	1.000±0.005	
14	0.993±0.008	0.7 %
15	0.912±0.008	
16	0.910±0.007	0.2 %

° the quoted errors are only the statistical one

LATTICE Nº 2

Fig: 4

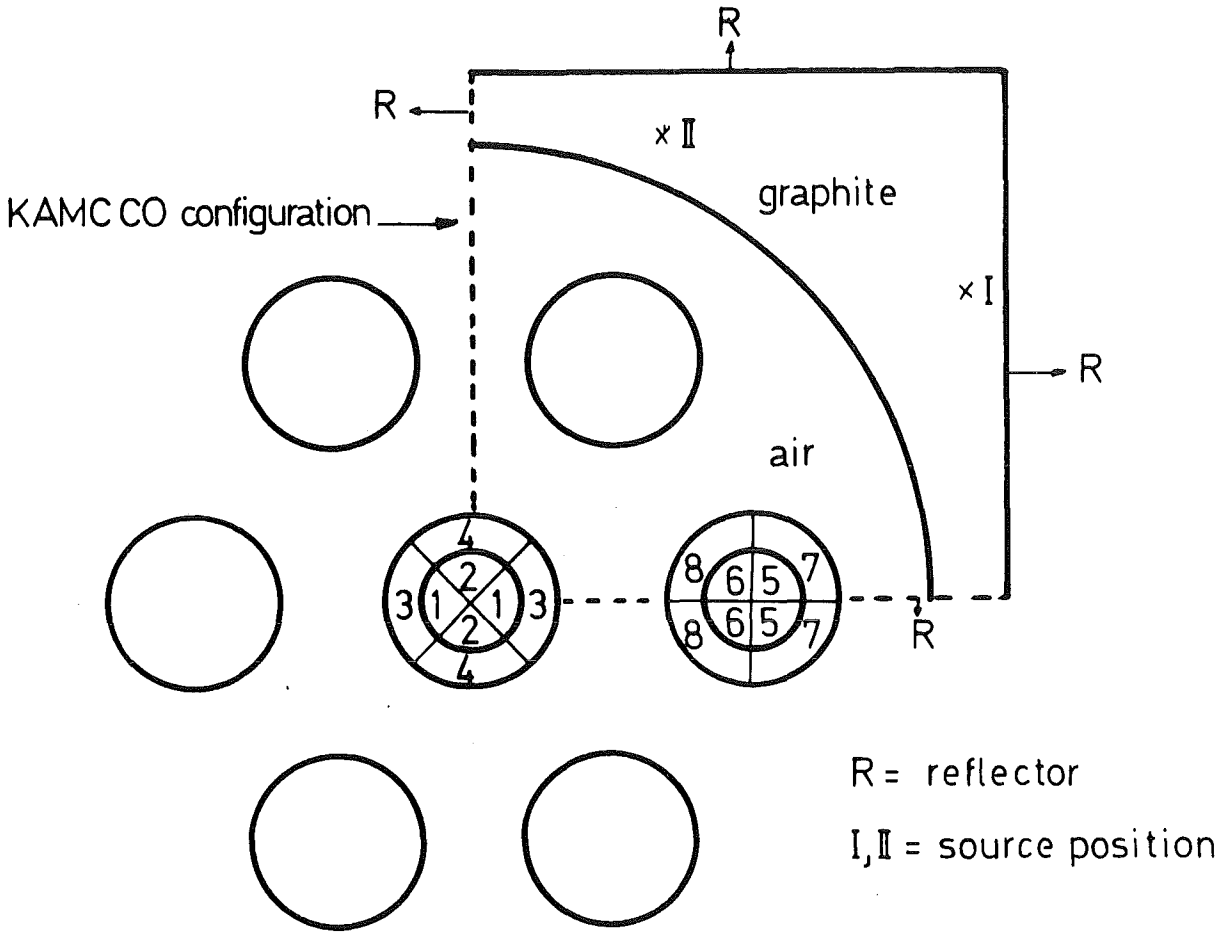

	KAMCCO (I)	KAMCCO (II)	KAMCCO average	Experiment
FR_1	0.987±0.026	0.989±0.026	0.988±0.018	0.987±0.008
FR_2	0.983±0.028	0.966±0.027	0.975±0.019	0.976±0.010
FR_3	1.031±0.024	1.025±0.024	1.028±0.017	1.016±0.007
FR_4	0.999±0.023	1.020±0.023	1.010±0.016	1.021±0.007
FR_5	0.988±0.021	0.986±0.021	0.987±0.015	1.000±0.005
FR_6	0.948±0.020	0.964±0.021	0.956±0.015	0.958±0.005
FR_7	1.088±0.019	1.077±0.020	1.083±0.014	1.067±0.006
FR_8	0.976±0.017	0.973±0.017	0.975±0.012	0.975±0.006

normalized to 1 for the pin

LATTICE Nº 2

Fig:5

Results

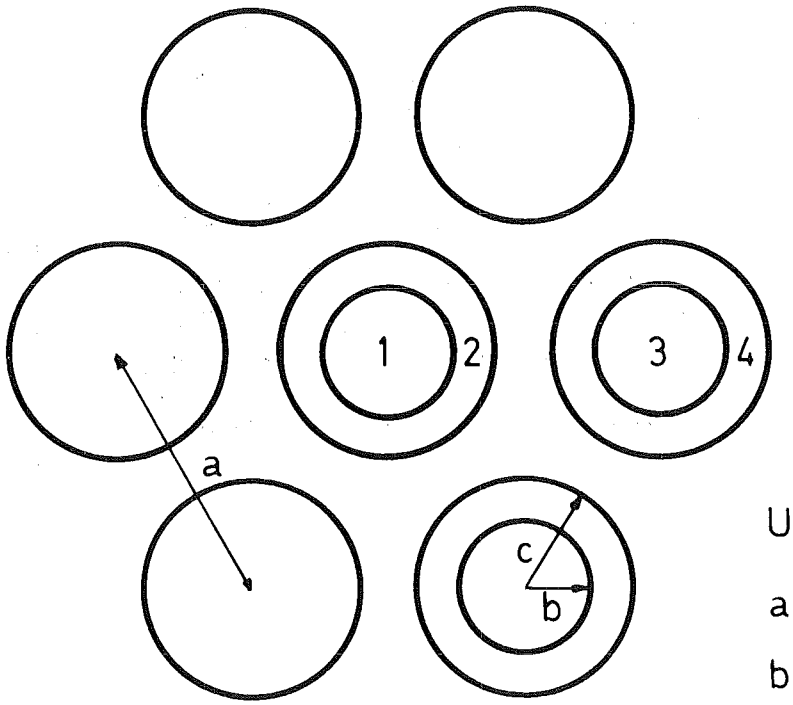

UO_2 (20%)

a = 0.9 cm

b = 0,211 cm

c = 0,345 cm

Fission Rate	Experiment	KAMCCO	WIMS
$FR_{1,2}$ °	0.946±0.008	0.945±0.009	0.951
$FR_{3,4}$ °	1.009±0.006	1.009±0.008	1.008
FR_1/FR_2	0.964±0.008	0.963±0.013	0.963
FR_3/FR_4	0.959±0.007	0.944±0.009	0.968

° normalized to 1.000 for the 7 pins

LATTICE Nº 3

Fig: 6

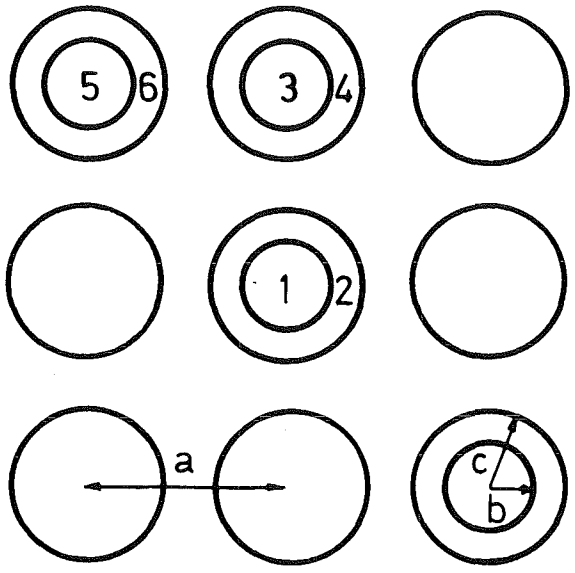

UO_2 (20%)

a = 0.9 cm

b = 0.211 cm

c = 0.345 cm

Fission Rate	Experiment	KAMCCO	WIMS
$FR_{1,2}$ +	0.934±0.007	0.926±0.011	0.939
$FR_{3,4}$ +	0.987±0.007	0.983±0.006	0.987
$FR_{5,6}$ +	1.029±0.006	1.038±0.006	1.028
FR_1 ++	0.986±0.007	0.984±0.015	0.982
FR_2 ++	1.014±0.006	1.016±0.012	1.018
FR_3 ++	0.981±0.006	0.976±0.008	0.985
FR_4 ++	1.019±0.006	1.024±0.007	1.015
FR_5 ++	0.976±0.005	0.969±0.008	0.983
FR_6 ++	1.024±0.005	1.031±0.006	1.016

\+ normalized to 1.000 for the 9 pins

++ normalized to 1.000 for the pin

LATTICE Nº4

Fig: 7

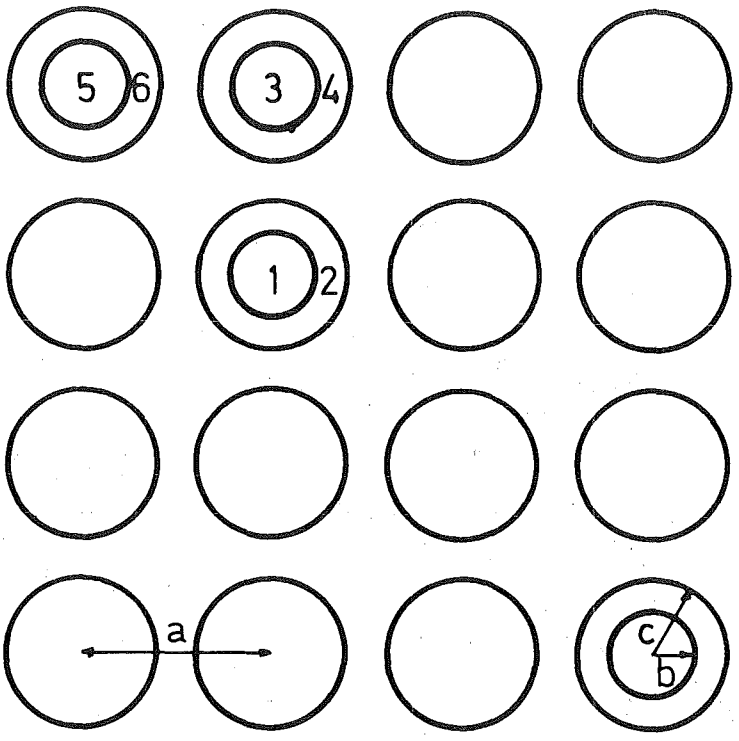

UO_2 (20%)

a = 0.9 cm

b = 0.211 cm

c = 0.345 cm

Fission Rate	Experiment	KAMCCO	WIMS
$FR_{1,2}$ +	0.921±0.008	0.914±0.007	0.923
$FR_{3,4}$ +	1.009±0.008	1.006±0.006	1.004
$FR_{5,6}$ +	1.061±0.008	1.069±0.007	1.069
FR_1 ++	0.987±0.006	0.986±0.009	0.987
FR_2 ++	1.013±0.006	1.014±0.008	1.013
FR_3 ++	0.981±0.008	0.971±0.007	0.986
FR_4 ++	1.019±0.008	1.029±0.006	1.014
FR_5 ++	0.976±0.008	0.970±0.008	0.985
FR_6 ++	1.024±0.008	1.030±0.006	1.015

\+ normalized to 1.000 for the 16 pins

++ normalized to 1.000 for the pin

LATTICE Nº 5

Fig: 8

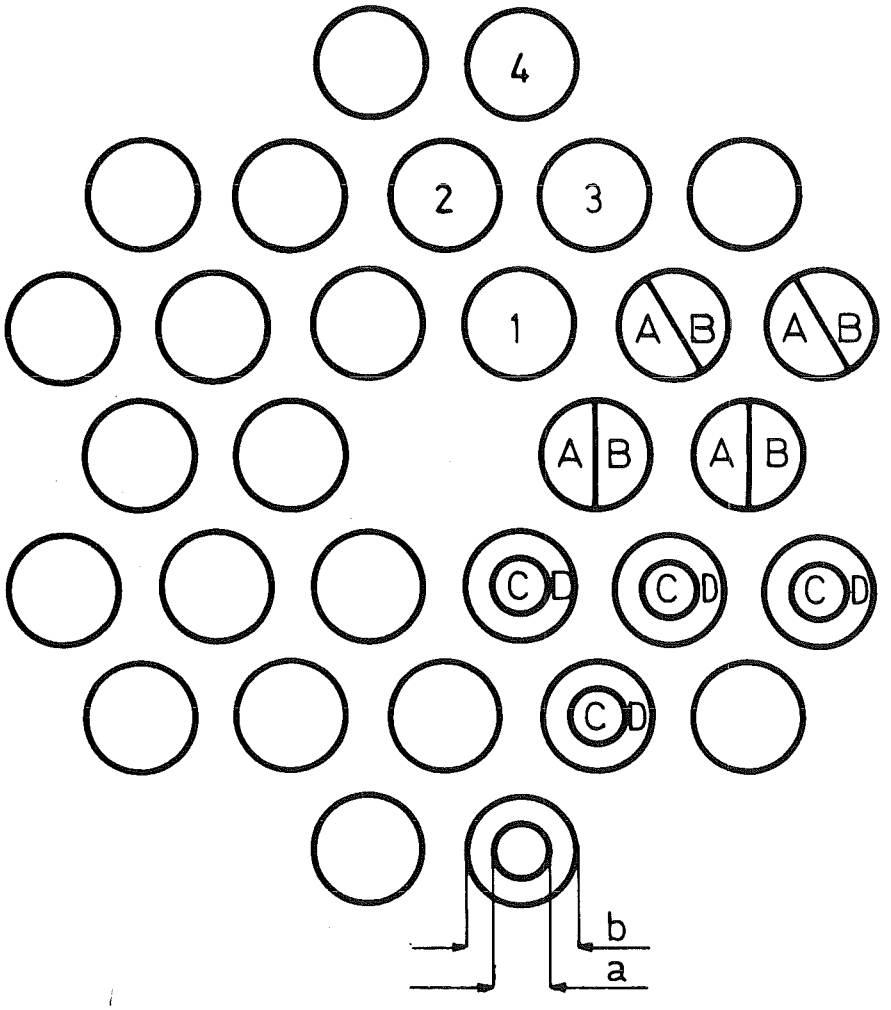

UO_2 (20% enriched)

pitch 1 cm

a = 0.211 cm

b = 0.345cm

Results Lattice No. 5 Fig: 9

Fission Rate	Experiment	KAMCCO	WIMS
FR_1 (1)	0.879±0.005	0.880±0.008	0.892
FR_2	0.946±0.005	0.948±0.008	0.953
FR_3	0.985±0.006	0.981±0.008	0.986
FR_4	1.095±0.006	1.096±0.007	1.085
FR_1^C (2)	0.986±0.006	0.991±0.011	0.990
FR_1^D	1.014±0.006	1.009±0.009	1.010
FR_2^C	0.983±0.006	0.986±0.010	0.991
FR_2^D	1.017±0.006	1.014±0.008	1.009
FR_3^C	0.981±0.005	0.985±0.008	0.990
FR_3^D	1.019±0.006	1.015±0.008	1.010
FR_4^C	0.971±0.005	0.969±0.007	0.989
FR_4^D	1.029±0.006	1.031±0.006	1.011
FR_1^A/FR_1^B	0.979±0.006	0.984±0.009	
FR_2^A/FR_2^B	0.945±0.006	0.939±0.009	
FR_3^A/FR_3^B	0.914±0.005	0.909±0.009	
FR_4^A/FR_4^B	0.898±0.005	0.892±0.008	

(1) normalized to 1.000 for the 30 pins

(2) normalized to 1.000 for the pin

LATTICE MOL-7B

Fig:10

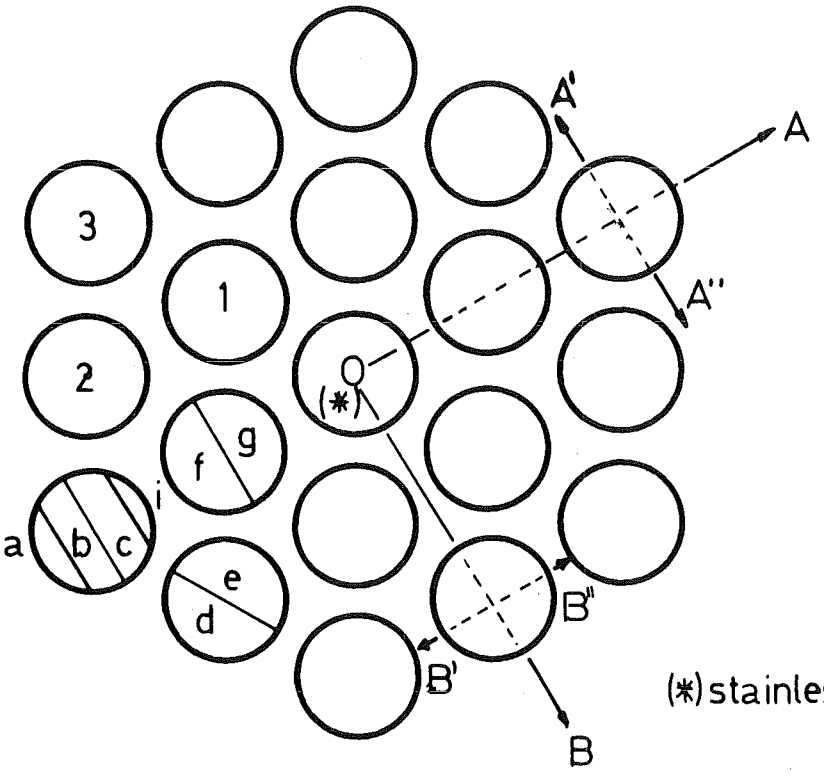

(*)stainless steel rod

material: UO_2- PuO_2

	Report MOL-7B (12)	KAMCCO
FR_1	0.875±0.009	0.883±0.008
FR_2	1.024±0.010	1.020±0.010
FR_3	1.102±0.011	1.086±0.010
FR_i/FR_a		0.746±0.020
$FR_{c,i}/FR_{a,b}$		0.853±0.013
FR_e/FR_d		0.875±0.016
FR_g/FR_f		0.956±0.015

The F.R. were normalized to 1.000 for the 18 pins

FIG : 11

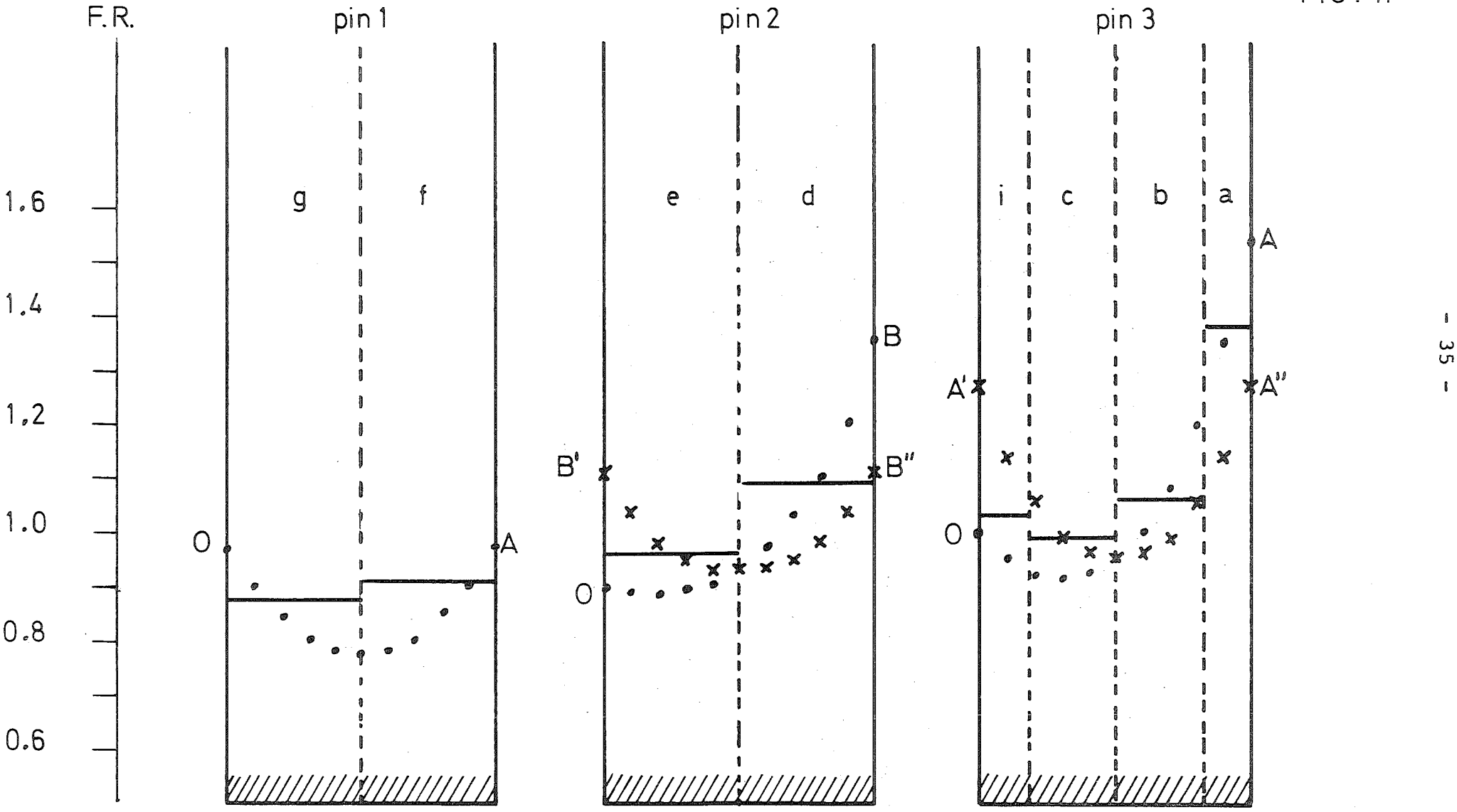

LATTICE MOL-7B
FISSION DENSITY DISTRIBUTION INSIDE THE FUEL PINS

x ∘ experiment (12)
— KAMCCO

LATTICE MOL-7C

Fig:12

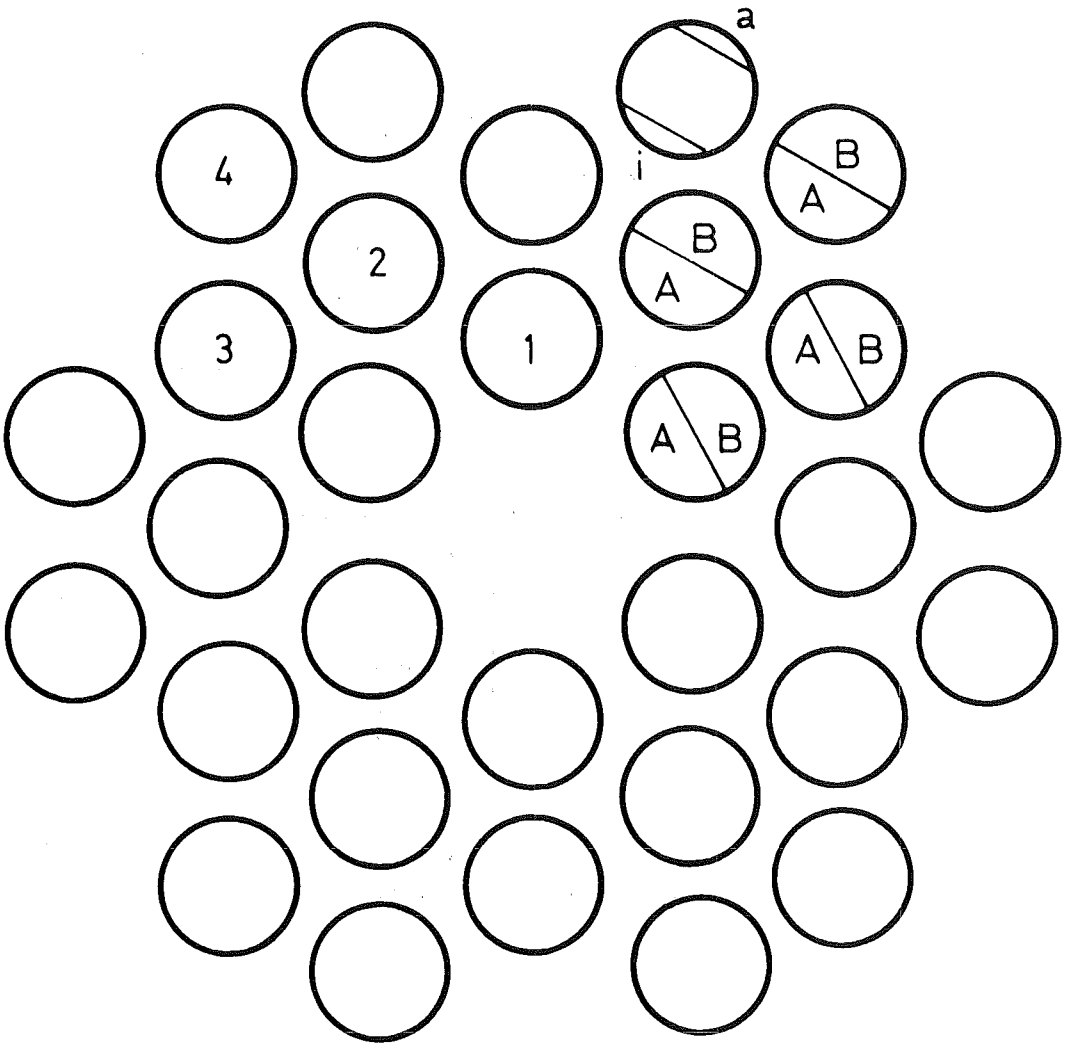

pitch = 0.79 cm

fuel composition UO_2

1 - 90 % enriched

2 - 80% enriched

3 - 80% enriched

4 - 65% enriched

FIG: 13

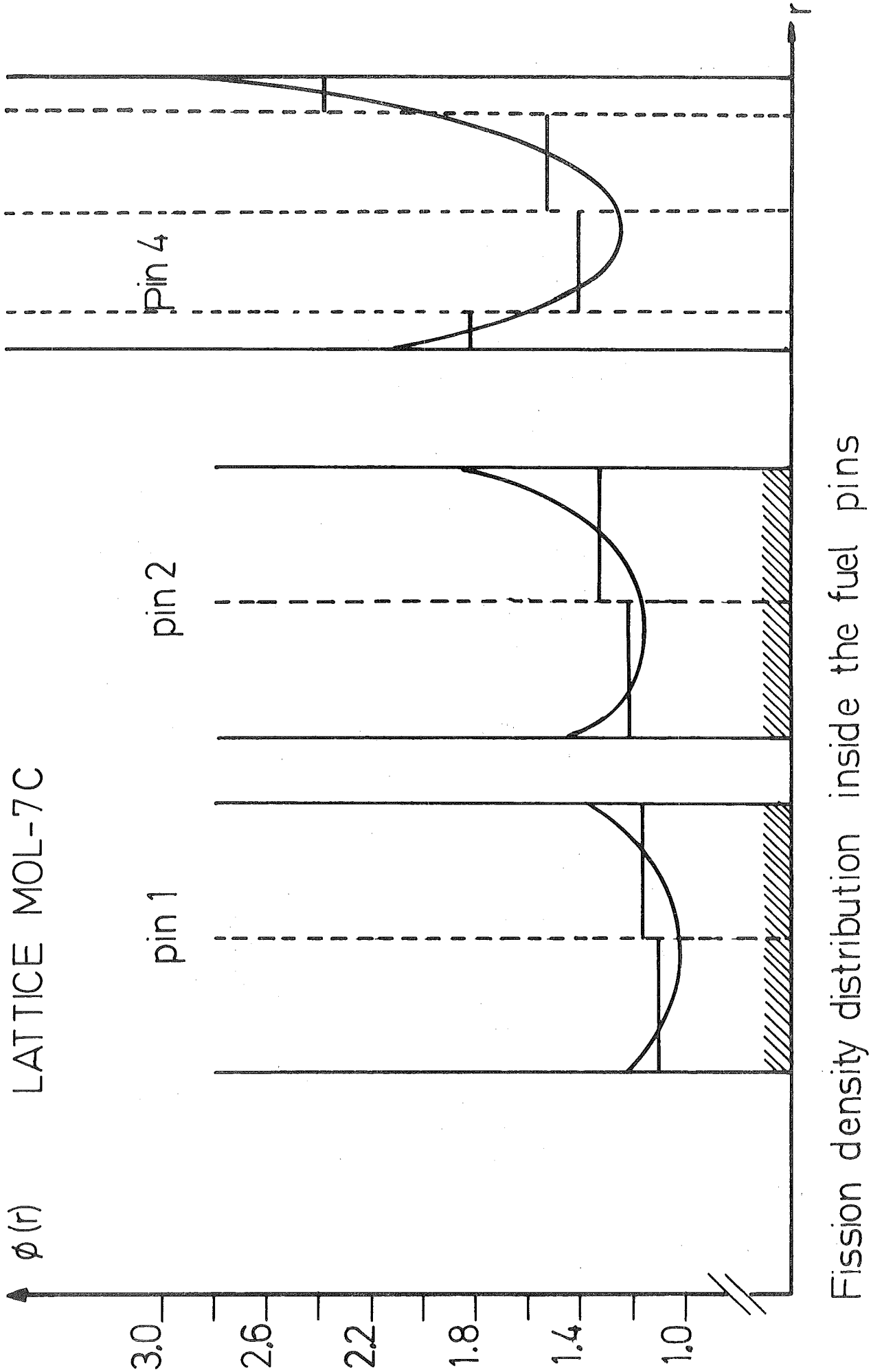

Fission density distribution inside the fuel pins

METHOD FOR COMPUTING FISSION RATIO FIG: 14

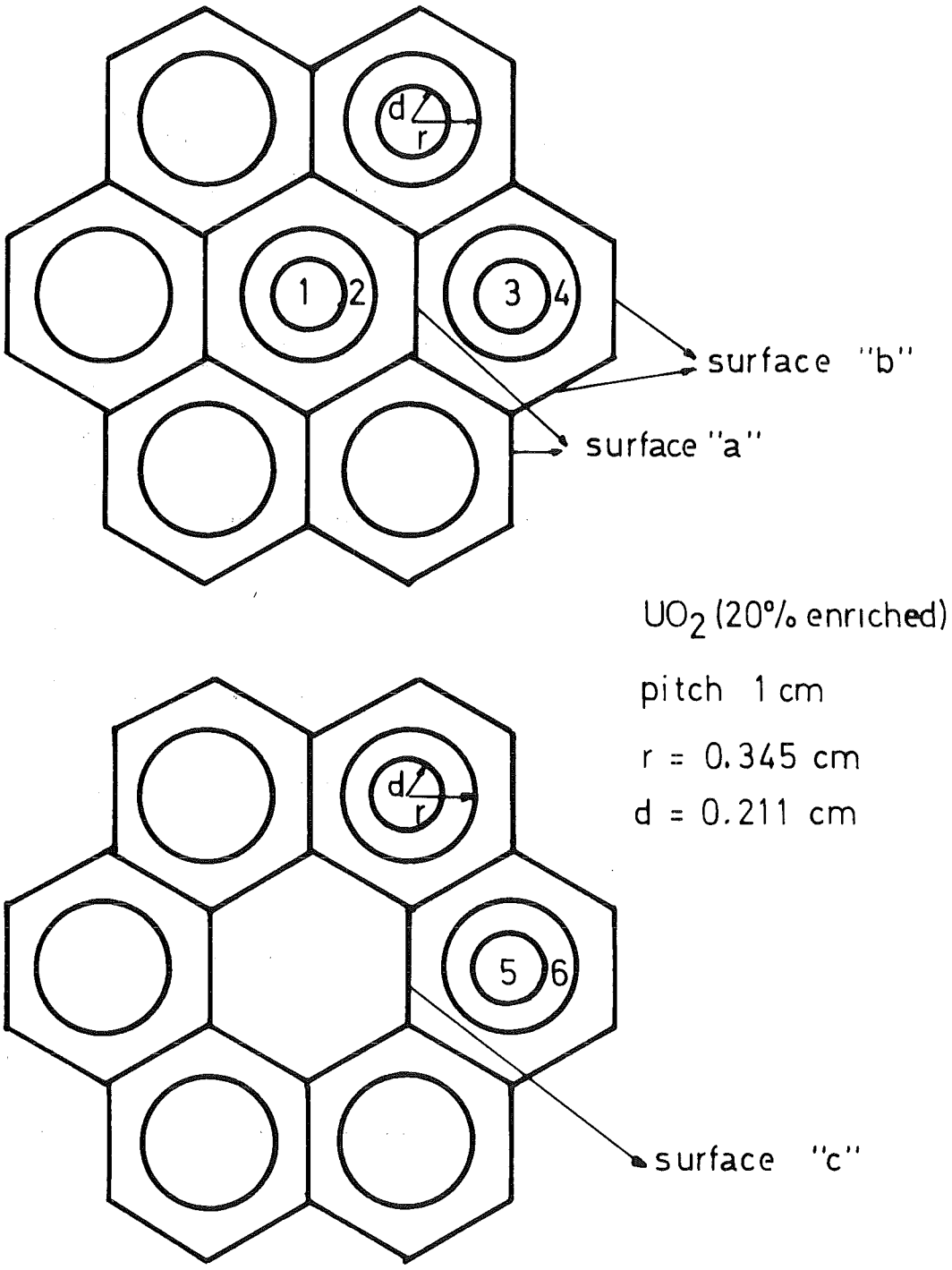

$R_A = FR_1 / FR_2$

$R_B = FR_3 / FR_4$

$R_C = FR_5 / FR_6$